



Research article

A method for robotic grasping based on improved Gaussian mixture model

Yong Tao^{1,2,*}, Fan Ren¹, Youdong Chen¹, Tianmiao Wang^{1,2}, Yu Zou³, Chaoyong Chen³ and Shan Jiang¹

¹ School of Mechanical Engineering & Automation, Beihang University, Beijing 100191, China

² Beijing Advanced Innovation Center for Biomedical Engineering, Beihang University, Beijing 100191, China

³ Wuhan University of Science and Technology, Wuhan 430081, China

* **Correspondence:** Email: taoy@buaa.edu.cn; Tel: +861082338271; Fax: +861082338271.

Abstract: The present research envisages a method for the robotic grasping based on the improved Gaussian mixture model. The improved Gaussian mixture model is a method proposed by incorporating Bayesian ideas into the Gaussian model. It will use the Gaussian model to perform grasping training in a certain area which we called trained area. The improved Gaussian models utilized the trained Gaussian models as prior models. The proposed method improved the cumulative updates and the evaluation results of the improved models to make robots more adaptable to grasp in the untrained areas. The self-taught learning ability of the robot about grasping was semi-supervised. Firstly, the observable variables of objects were determined by a camera. Then, we dragged the robot to grasp object. The relationship between the variables and robot's joint angles were mapped. We obtained new samples in the close untrained area to improve the Gaussian model. With these new observable variables, the robot grasped it successfully. Finally, the effectiveness of the method was verified by experiments and comparative tests on grasping of real objects and grasping simulation of the improved Gaussian models through the virtual robot experimentation platform.

Keywords: robotic grasping; improved Gaussian models; V-REP simulation

1. Introduction

Currently, the utility of robots in fulfilling various tasks in place of human beings in industrial

production and daily life is gaining a significant importance. For instance, robots outperform human beings in many operations like welding, cutting, punching, paint spraying, treatment of heavy materials and sophisticated material processing [1]. In the grasping operations of the robots, frequent changes are associated in the poses of the target objects. To make robotic grasping more adaptive, robots have to regulate their motions on a real-time basis based on the information about object poses.

At present, more studies focus on the robotic grasping based on machine visions. Firstly, the vision-based robots need to visually determine the poses of objects. Then, coordinates of robots' joints are determined through inverse kinetics. At last, the motions of the robots are planned by the designed motion planner. In this process, it is necessary to calibrate the visual systems. The operators need to be highly professional by traditional visual calibration methods [2–4]. Meanwhile, the computations involved in the process are very time-consuming. Besides, it is difficult to determine the inverse solutions for robots with new structures or redundant degrees of freedom. Finally, the planner design is a little complicated, which may cause other problems.

Researchers satisfied the present needs for robotic grasping by different methods; some studies were devoted to equip the end actuators with sensors such as tactile feedbacks [5], while some studies improved the end actuators to make robots more adaptive to grasping, for instance, D. Petković presented a novel design of an adaptive neuro fuzzy inference strategy (ANFIS) for controlling the input displacement of a new adaptive compliant gripper [6]. The use of embedded sensors in a robot gripper offered the control system, the ability to control the input displacement of the gripper and to recognize particular shapes of the grasping objects. Some studies focused on increasing the underactuated degree of freedom [7], and some studies used flexible materials [8] to manufacture more flexible end actuators. C. Qian et al. designed the robotic arms with 12 degrees of freedom based on multi-sensor fusion [9]. In these robotic arms, the sensors were used in combination with the controllers. It presented general shapes of objects through information fusion, and endowed the robotic arms with bionic functions. In consideration of the considerable costs in motor control and poor control precision of the robotic arms, S. Liu et al. designed the STM32-based robotic arms [10]. In this way, problems such as inaccurate motor positioning and considerable costs were effectively avoided. In addition, these robotic arms could be controlled more easily and flexibly. Although, the aforementioned methods are effective for increasing adaptivity of the robots' end actuators, they are only useful for robots to grasp objects within the scope of work of the end actuators.

Many researchers identified the poses of objects visually and adjusted the robots' motions for the purpose to grasp objects. Saxena et al. identified the positions and shapes of the target objects by analyzing several images of the objects, so as to draft suitable strategies for robotic grasping [11]. W. Dong introduced the computer visions in the original industrial transport robots [12]. They obtained information about the workpieces and surroundings by machine vision. Then, they identified the target workpieces to be operated and made decisions to guide the industrial robots to grasp and place workpieces.

Currently, more and more researchers have introduced the “intelligence” into grasping. They performed deep learning and training for robotic arms and gained some outcomes. Z. Yan et al. proposed a method for detecting the robots' grasping positions based on deep learning [13]. In this method, the multimodal features of the target objects were employed as the training data. Robots learnt about the optimal grasping positions of target objects through unsupervised and supervised

learning. In this way, they could accurately identify the optimal grasping positions of the target objects. Xia Jing put forward a rapid detection method of robot's plane grabbing posture based on cascade convolutional neural network [14]. He built a cascaded two-stage convolutional neural network model and used transfer learning to train models on small data sets. The results of online robotic grasping experiments showed that the method can quickly calculate the optimal grasping point and pose for irregular objects with arbitrary poses and different shapes. Its recognition accuracy and speed are improved compared with previous methods, and its robustness and stability are strong.

Robots can acquire skills for fulfilling the tasks from the people's presentations. Y. Mollard [15] made a rapid and intuitive programming by demonstration of robot. K. Bousmalis [16] studied the effect of the randomized simulated environments and domain adaptation methods in training a grasping system to grasp novel objects from raw monocular RGB images. As a result, they were able to reduce the number of real-world samples needed to achieve a given level of performance, by up to 50 times. Max Schwarz et al. proposed a deep object perception pipeline [17]. This method quickly and efficiently adapted to the new items using a custom turntable capture system and transfer learning. It produced high-quality item segments, on which grasp poses were found. Philipp Schmidt presented a data-driven, bottom-up, deep learning approach to robotic grasping of unknown objects using Deep Convolutional Neural Networks (DCNNs) [18]. They demonstrated the performance of our approach in qualitative grasping experiments on the humanoid robot ARMAR-III.

Earlier, we proposed a robot demonstration method based on the combination of locally weighted regression (LWR) and Q-learning algorithm [19]. This method adapted to the work task by learning from the demonstration and generating new actions. In literature [20], we built models in the Gaussian process to develop the relationship between the observable variables and the joint variables. Then the robot was able to adaptively grasp the target objects. However, adaptive grasping is only realized within relatively small training areas when models are built in a Gaussian process. If an area for object distribution is enlarged and extends to the untrained area, the effectiveness of this modelling method for robotic grasping gets greatly weakened, and the success rate of robotic grasping, in turn, gets lower.

In view of these problems, this paper proposes a robotic grasping method based on the improved Gaussian mixture models. The coordinates of the targets were extracted through a camera to get some samples for teaching. The relationships between observable variables and robots' joint angles were mapped by the improved Gaussian models. Furthermore, the Gaussian models gained via training were used as prior models and integrated into the process of semi-supervised self-taught learning. By self-taught learning of grasping, robots grasped objects in new adjacent areas and new training samples were collected. Then we updated the probability distribution of the entire Gaussian process, obtained the posterior probabilistic models and achieved a higher success rate of grasping. For this purpose, models were built for simulation based on V-REP [21–23]. Then, they were compared with the original and improved Gaussian models in success rate of grasping. Besides, test areas where grasping by all three methods failed were analyzed in terms of positional deviation. At last, it was found that the improved Gaussian models were more adaptive.

2. Gaussian model and EM algorithms

Gaussian model precisely quantifies things using Gaussian probability density functions (normal distribution curves). It decomposes one thing into several Gaussian probability density

functions (normal distribution curves).

The Expectation-Maximization (EM) algorithms are optimal algorithms for the estimation of the maximum likelihood. In general, they are used in place of the Newton’s iteration. Meanwhile they are used for estimating the parameters of the probabilistic models containing latent variables or missing data. The standard computational framework for EM algorithms is alternately composed of E and M steps. The algorithms are convergent, so they are useful for ensuring that iteration can at least approach local maximum.

Robots have to regulate themselves to adapt to objects in the process of grasping.

$$f : o \rightarrow r \tag{1}$$

In Figure 1 and Formula (1), o is an observable variable of objects, so is o_i ; r is robot’s joint variable corresponding to the observable variable, so is r_i ; f is mapping of the observable variable into the joint variable. Assuming that $X = \{x_1, x_2, \dots, x_n\}$ is a set of training samples obtained through demonstration, where $x_i = [r_i, o_i]^T$ is a single training sample (vector) made up of joint variables and observable variables. In the process of its work, the robot firstly learn from the set of training samples (X) to get the mapping function (f); when the new observable variable (o^{new}) is determined, corresponding joint variable (r^{new}) is calculated based on the mapping function (f).

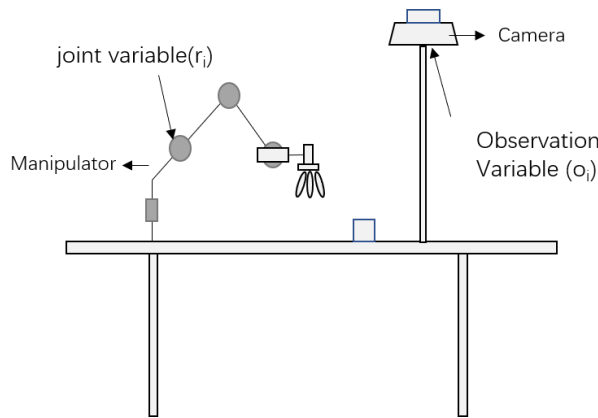


Figure 1. Observable variables and joint variables.

Selecting a suitable model to describe the mapping function (f) is fairly suitable for robots to learn about grasping. In this paper, modelling was performed by the improved Gaussian mixture models, to map the relationships between the observable variables of objects and the joint variables of robots. The models were trained with EM algorithms, and training samples were divided into several categories. Each type of samples followed a kind of Gaussian distribution and corresponded to one area.

A Gaussian mixture model was a linear superposition of several Gaussian distributions. For probability distribution of a Gaussian mixture model, the appearance probability of the sample x^o is as follows:

$$p(x^o) = \sum_{k=1}^m p(k) p(x^o | k) = \sum_{k=1}^m a_k N(x^o; \mu_k, \Sigma_k) \tag{2}$$

Where, m is total number of Gaussian distributions; $p(k) = \alpha(k)$ is the probability of the k^{th}

Gaussian distribution from the sample x^o ; $p(x^o/k)=N(x^o;\mu_k;\Sigma_k)$ is the probability of the sample x^o generated by the k^{th} Gaussian distribution; μ_k and Σ_k are mean vector and covariance matrix of the k^{th} Gaussian distribution respectively.

Samples were trained by EM algorithms of Gaussian mixture models and categorized. A work area was designated for each kind of samples. The relationships between observable variables of objects and joint variables of robots were mapped. After model parameters were initialized, E-step and M-step were iterated to constantly update model parameters until they are converged:

E-step: calculate the weight (r_{ik}) of the k^{th} Gaussian distribution from the i^{th} sample (x_i).

$$r_{ik} = p(k | x_i) = \frac{\alpha_k N(x_i; \mu_k, \Sigma_k)}{\sum_{j=1}^m \alpha_j N(x_i; \mu_j, \Sigma_j)} \quad (3)$$

M-step: update parameters of each cluster.

$$\begin{aligned} n_k &= \sum_{i=1}^n r_{ik}, \alpha_k = \frac{n_k}{n} \\ \mu_k &= \sum_{i=1}^n r_{ik} x_i \\ \Sigma_k &= \frac{\sum_{i=1}^n r_{ik} (x_i - \mu_k)(x_i - \mu_k)^T}{n_k} \end{aligned} \quad (4)$$

While robots were grasping objects based on improved Gaussian model, the observable variables of the objects were identified through a camera to calculate the posterior probability of these variables in each Gaussian distribution. The robots' joint coordinates were determined by a regression of the improved Gaussian process corresponding to the maximum posterior probability. Then robots were able to grasp the objects successfully.

3. Control methods for robotic grasping based on improved Gaussian models

3.1. Principles of robotic grasping methods based on improved Gaussian models

Principles of robotic grasping methods based on improved Gaussian models are shown in Figure 2:

(1) Relationships between observable variables of target objects and corresponding robots' joint variables were mapped using original Gaussian models. Then we identified the overall mapped relationships based on data regarding 12 groups of samples.

(2) Target positions were randomly selected in new training areas as inputs of Gaussian processes. Joint angles were predicted as the outputs. In simulation models, positive solutions were determined on the basis of joint angles. Positions of the corresponding pixel coordinates at ends of robots were observed and recorded. If the predicted and actual positions deviated by Δd less than 10 mm, the newly determined robots' joint angles were regarded as new samples to input and update the training sets of Gaussian processes, in order to update the entire distribution process. When cumulative values reached the thresholds, it meant that enough samples were additionally obtained from the new training areas. Then posterior Gaussian distribution in the new training areas was identified.

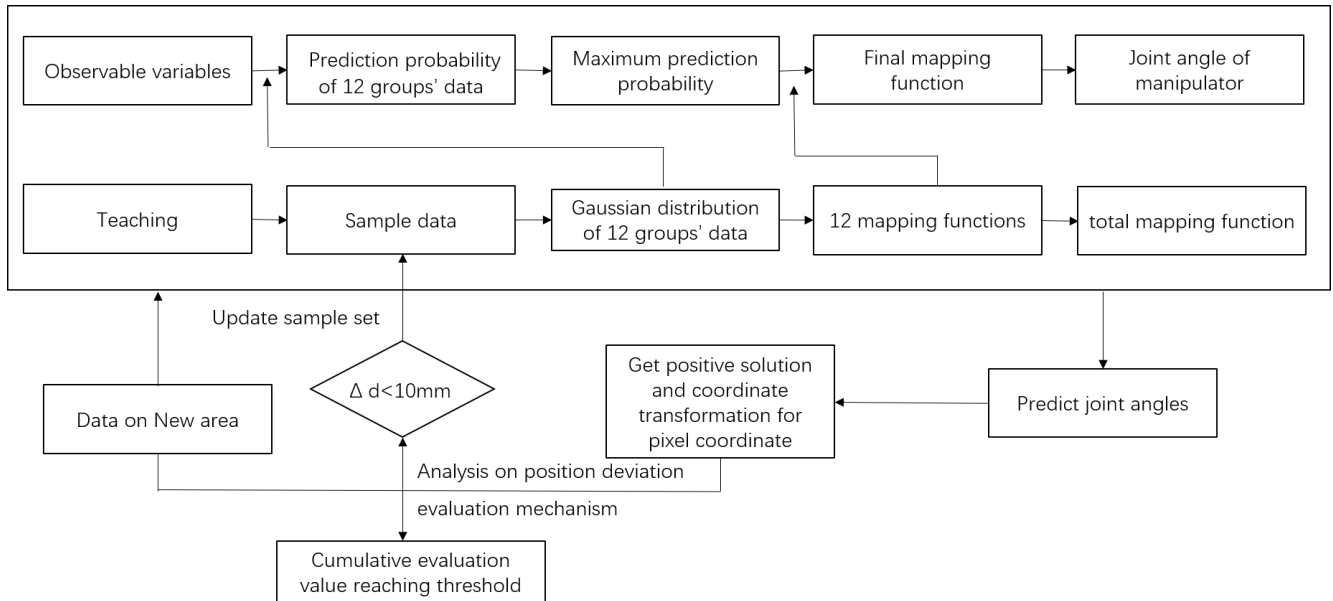


Figure 2. Robotic grasping methods based on improved Gaussian models.

3.2. Control Methods for Robotic Grasping Based on Improved Gaussian Models

Gaussian process modelling (GPM) method is a hypothesis for following joint normal distribution based on observable and predicted variables. We use it to calculate observable variables. Posterior probability distribution can be identified by a random input covariance matrix for training machines. GPM is a Bayesian approach, by which robots can get mapping functions from samples f . For a minority of samples, Gaussian process models can be trained. Then nonlinear connections of related variables are created.

Before data are obtained, it is assumed that joint variables and observable variables of objects follow Gaussian distribution, where the mean is μ and the covariance matrix is K :

$$h: N(\mu, K) \quad (5)$$

Where, $h = [a, o]^T$ is a vector composed of observable variables and joint variables.

Meanwhile, the posterior distribution of multi-dimensional variables obtained for the sample set X is Gaussian distribution:

$$p(h|X, \theta) = N(\mu, K + \sigma_n^2 I) \quad (6)$$

Where, $\theta = \{\mu, K, \sigma_n^2\}$ The marginal likelihood function of the sample set X is as follows:

$$p = (X|H, \theta) = \prod_{(i=1)}^n p(x_i|h_i, \theta) = \prod_{(i=1)}^n p(x_i|h_i)p(h_i|\theta) = P \quad (7)$$

Where:

$$P = \prod_{(i=1)}^n \frac{1}{\sqrt{2\pi |K + \sigma_n^2 I|}} \exp\left(-\frac{\tau_i}{2}\right) \quad (8)$$

$$\tau_i = (x_i - \mu)^T (K + \sigma_n^2 I)^{-1} (x_i - \mu) \quad (9)$$

The logarithm of the above formula is determined as follows:

$$\log(P) = A + B - \frac{n}{2} \log(2\pi) \quad (10)$$

Where:

$$A = -\frac{1}{2} \sum_{(i=1)}^n \tau_i \quad (11)$$

$$B = -\frac{n}{2} \log |K + \sigma_n^2 I| \quad (12)$$

A and B are fitted data of the model and penalty term of model complexity respectively.

By determining partial derivatives of covariance matrix and mean vectors of the mode, the derivatives were found to be 0. The maximum likelihood estimations of the mean vectors and covariance matrix are respectively as follows:

$$\mu = \frac{\sum_{(i=1)}^n x_i}{n} \quad (13)$$

$$(K + \sigma_n^2 I) = \text{Cov}([x_1, x_2, \dots, x_n]^T) \quad (14)$$

Next, it is necessary to forecast joint variables using Gaussian process models. The relationships between visual observable variables and joint variables shall be established based on teaching and training samples. At first, vectors and matrices of the Gaussian process are partitioned as follows:

$$\begin{bmatrix} a \\ o \end{bmatrix} : N \left[\begin{bmatrix} \mu_a \\ \mu_o \end{bmatrix}, \begin{bmatrix} K_{aa} + \sigma_n^2 I & K_{ao} \\ K_{oa} & K_{oo} + \sigma_n^2 I \end{bmatrix} \right] \quad (15)$$

Robots acquire information O^* about target objects through a camera, and the conditional probability distribution of corresponding joint angle a^* is as follows:

$$p(a^* | o^*) = N(\mu_a^*, K_{aa}^*) \quad (16)$$

Where:

$$\mu_a^* = \mu_a + K_{ao} (K_{oo} + \sigma_n^2 I)^{-1} (o^* - \mu_o) \quad (17)$$

$$K_{aa}^* = K_{aa} - K_{ao} (K_{oo} + \sigma_n^2 I)^{-1} K_{oa} \quad (18)$$

μ_a^* is the mean of joint angle corresponding to the new target position. It is the maximum probability of corresponding Gaussian distribution meanwhile. The covariance matrix is K_{aa}^* , which reflects predictive uncertainty. If robot joint is μ_a^* , the likelihood of robotic grasping will be the highest.

By reading data of the controller, relatively accurate joint coordinates of robots are determined as follows:

$$K_{aa}^* \approx (K_{aa}^* + \sigma_n^2 I) = K_{aa} + \sigma_n^2 I - K_{ao} (K_{oo} + \sigma_n^2 I)^{-1} K_{oa} \quad (19)$$

In case of no visual calibration and inverse kinematic solution, target objects of the Gaussian process are closely associated with joint variables. Therefore, robots' joint angles adaptable to target poses can be forecast according to observable variables.

The obtained Gaussian process models are deemed prior models. New models are built for the grasping in new trained areas by improved Gaussian methods. The equation is as follows:

$$p(\theta | X) = \frac{p(X | \theta) \cdot p(\theta)}{p(X)} \quad (20)$$

Where $p(\theta)$ is probability distribution of prior models; X is training sample; $p(\theta|X)$ is probability distribution of posterior models; $p(X)$ is marginal likelihood. By the following equation, it is calculated that:

$$p(X) = \int p(X | \theta) p(\theta) d\theta \quad (21)$$

The Gaussian methods were improved for the purpose of expanding new application areas without excessively increasing sample points of original models. Therefore, this paper introduced an evaluation mechanism, in order that improved models could have expected functions after certain amount of sample points were updated. A mechanism was established for evaluating grasping in combination with the actual grasping positions. The actual positions were identified based on target positions and posterior models, so as to figure out termination requirements for posterior models. Evaluation functions were determined as follows:

$$r = S_r e^{-\lambda \Delta d} + S_r', \Delta d = \sqrt{(x_a - x_d)^2 + (y_a - y_d)^2} \quad (22)$$

Where, S_r is the evaluated value when Δd is 0; λ is a parameter for ensuring convergence of $e^{-\lambda \Delta d}$ to 0 when Δd is high enough. S_r' is the value evaluated after another new sample is used.

The termination requirements for completing updates of areas are as follows:

$$R = \sum_{(i=1)}^n r_i > \kappa \quad (23)$$

In other words, the new area shall be deemed to have been updated when the cumulative evaluated value reaches certain threshold.

4. Experiments

4.1. Building of the experimental platform

This robotic grasping system covered data acquisition, data processing and industrial robots, as shown in Figure 3. A UR3 robot was used. It had six spindles from the bottle to the end, including base, shoulder joint, elbow joint, wrist joint 1, wrist joint 2 and wrist joint 3. MV-EM200C/M camera was used and its resolution was 1,600*1,200. The gripper at the end was a motor-driven three-finger gripper with a single degree of freedom.

The experimental platform was configured as shown in Figure 4. The camera was placed above the platform. UR3 robot was on the experimental platform. The block was in the area near the black cloth. The block to be grasped was a small cube. By determining the mean of the coordinates of edge

points of the block, the pixel coordinates x and y in the centre of the object were identified, as shown in Figure 5.

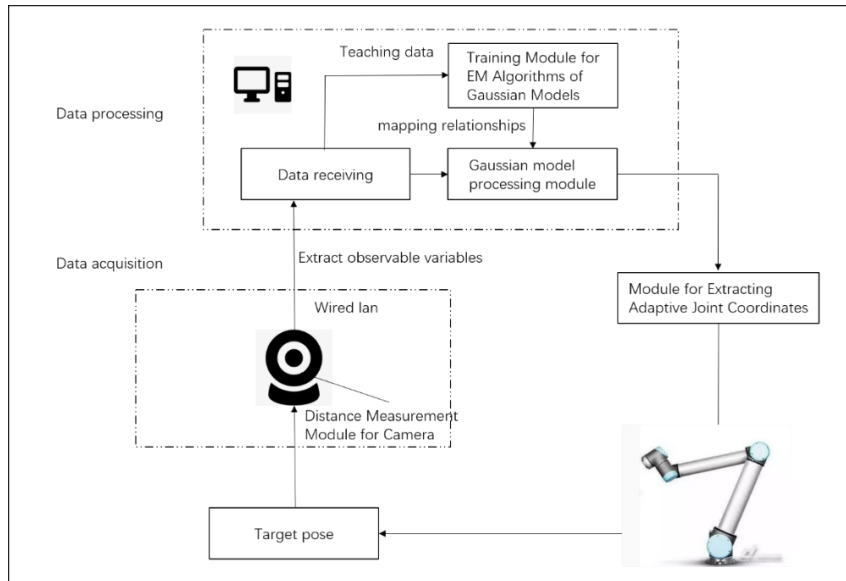


Figure 3. System components.



Figure 4. Configuration of the experimental platform.

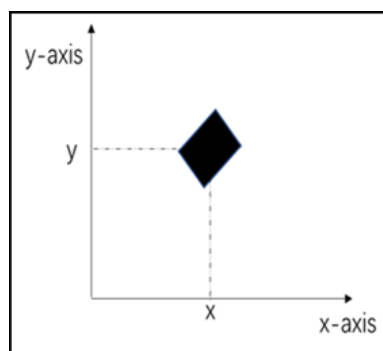


Figure 5. Poses of the target objects.

4.2. Grasping experiment based on improved Gaussian models

The experimenter dragged the robot to the position of each block to determine the joint angles. Pixel coordinates of the blocks were obtained through a camera. Twelve experiments were performed. At last, obtained data of the observable variables and joint angles were used as training samples of models. Joint angles and pixel coordinates of the robot was recorded and utilized as training samples and input for the Gaussian process models, as shown in Table 1.

Table 1. Set of training samples.

No.	Observable Variables		Corresponding Joint Coordinates (Radian)					
	Pixel (x)	Pixel (y)	Base	Shoulder Joint	Elbow Joint	Wrist Joint 1	Wrist Joint 2	Wrist Joint 3
1	239	88	-0.134	-1.730	-2.022	-0.965	1.573	0.007
2	347	88	0.003	-1.661	-2.103	-0.951	1.574	0.145
3	455	87	0.149	-1.609	-2.161	-0.944	1.575	0.291
4	455	191	0.130	-1.768	-1.976	-0.970	1.574	0.271
5	347	192	0.003	-1.810	-1.920	-0.985	1.573	0.145
6	239	192	-0.118	-1.868	-1.841	-1.008	1.572	0.023
7	239	297	-0.105	-2.004	-1.639	-1.073	1.571	0.036
8	347	297	0.003	-1.953	-1.717	-1.045	1.572	0.144
9	454	296	0.116	-1.917	-1.772	-1.026	1.573	0.257
10	401	244	0.062	-1.861	-1.852	-1.003	1.573	0.204
11	293	245	-0.055	-1.907	-1.785	-1.024	1.572	0.086
12	293	140	-0.062	-1.767	-1.977	-0.973	1.573	0.079

After training samples were obtained, the mean vector of the Gaussian process μ and the maximum likelihood estimation of covariance matrix ($\mathbf{K} + \delta_n^2 \mathbf{I}$) were determined. The new observable variables and robot's joint coordinates followed the same probability distribution. In case, if there was any new observable input \mathbf{o}^* , the joint angles μ_a^* were obtained that the robot was most likely to grasp at, so as to make grasping successful.

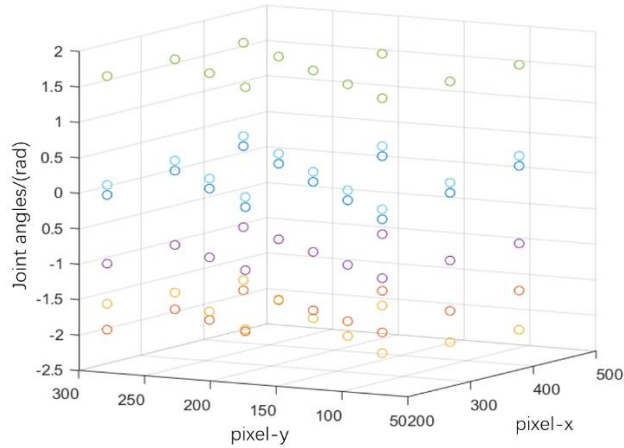


Figure 6. Joint angles of the training samples and corresponding pixel coordinates.

Figure 6 shows the pixel coordinates and the corresponding joint angles of training samples. The joint angles of the base, shoulder joint, elbow joint, wrist joint 1, wrist joint 2 and wrist joint 3 were allocated from the bottom to the top. Figure 7 shows the distribution and grasping status of the training samples and the test samples on the pixel plane. The squares represent the training samples, hollow circles were successfully grasped test samples, and the solid circles were the test samples that were not successfully grasped. It is evident from the figure that the Gaussian models were helpful in the successful grasping in areas within the set of the training samples, but the grasping always failed outside the training areas. Hence, it is inferred that the Gaussian process models function fairly well within the training areas. The grasping results were not satisfactory on the boundaries near the training areas and test points outside the training areas. This suggested that the Gaussian process models were reliant upon the prior samples and were able to function well without these samples. This is a limitation of Gaussian models.

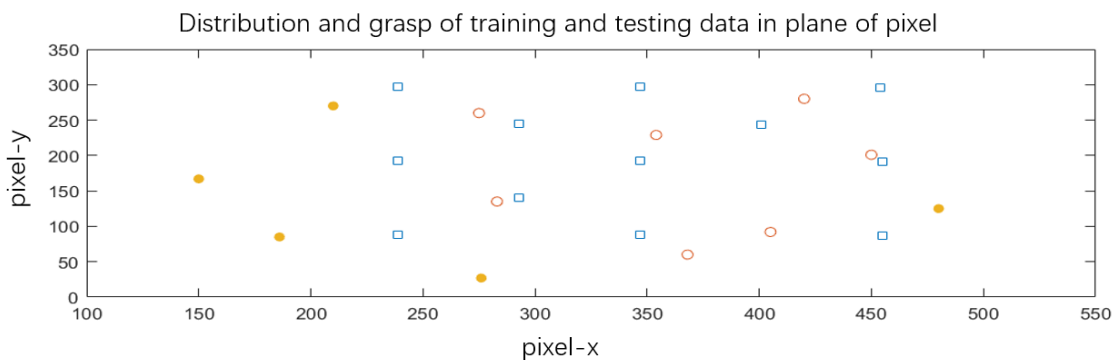


Figure 7. Planar distribution of pixels and grasping status of training and test samples.

Sample points of new areas were cumulatively updated by the improved Gaussian models. We selected points conforming to $\Delta d < 10$ mm as new samples for updating sample sets and calculated the evaluated values, until they reached the thresholds. This experiment suggested that only six new

data were needed, and this number was far lower than the number of training samples necessary for the original Gaussian models.

Table 2. New sample set.

No.	Pixel (x)	Pixel (y)	Position Error (Δd)	Base	Shoulder Joint	Elbow Joint	Wrist Joint 1	Wrist Joint 2	Wrist Joint 3
1	560	88	5.26	0.253	-1.568	-2.232	-0.912	1.576	0.395
2	668	192	1.63	0.378	-1.662	-2.107	-0.942	1.576	0.520
3	560	192	8.86	0.252	-1.713	-2.041	-0.960	1.575	0.394
4	722	244	8.64	0.440	-1.709	-2.045	-0.957	1.576	0.582
5	615	245	4.02	0.316	-1.761	-1.977	-0.975	1.575	0.458
6	614	140	7.57	0.315	-1.615	-2.170	-0.927	1.576	0.457

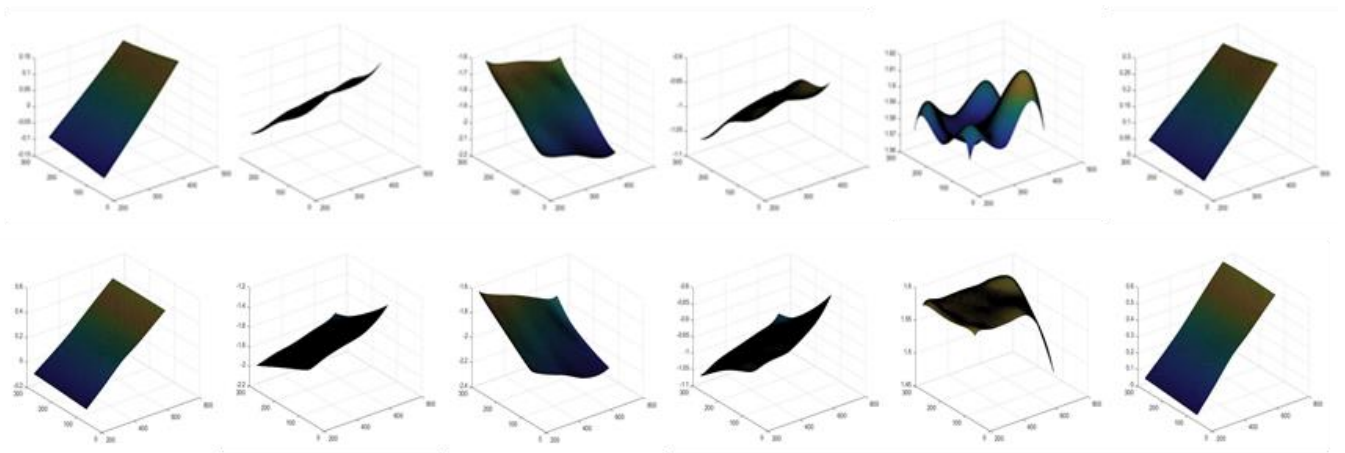


Figure 8. Distribution of joint angles.

Figure 8 shows distribution of the robot's joint angles. The first row lists the joint angles of the original Gaussian model, while the second row shows the joint angles that were determined after the update of six sample points. It is evident that changes occurred to these joint angles. In particular, these changes were rather significant for the wrist joints 2 and 3, which suggested that the joint angles for grasping changed considerably in the new mapping relationships after the update.

In order that the experiment could be accurate and generalized, this paper modelled and simulated the grasping based on VREP. As shown in Figure 9, The UR3 and blocks were put on the table and a camera was placed above them. We compared the success rate of the grasping among the original Gaussian model for grasping real objects, the improved Gaussian model for grasping simulation based on VREP and the improved Gaussian model for grasping real objects, as shown in Figures 10–12.

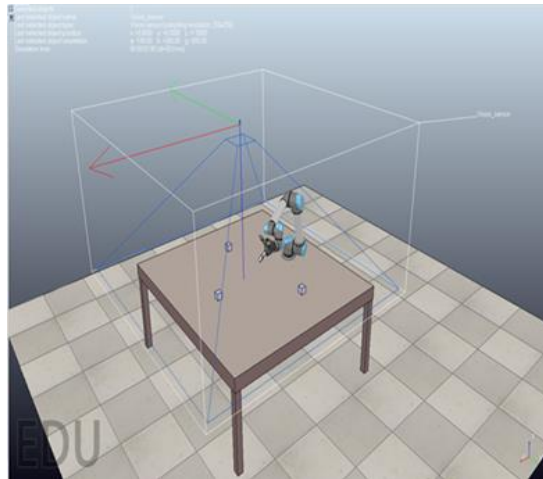


Figure 9. V-REP based simulation platform.

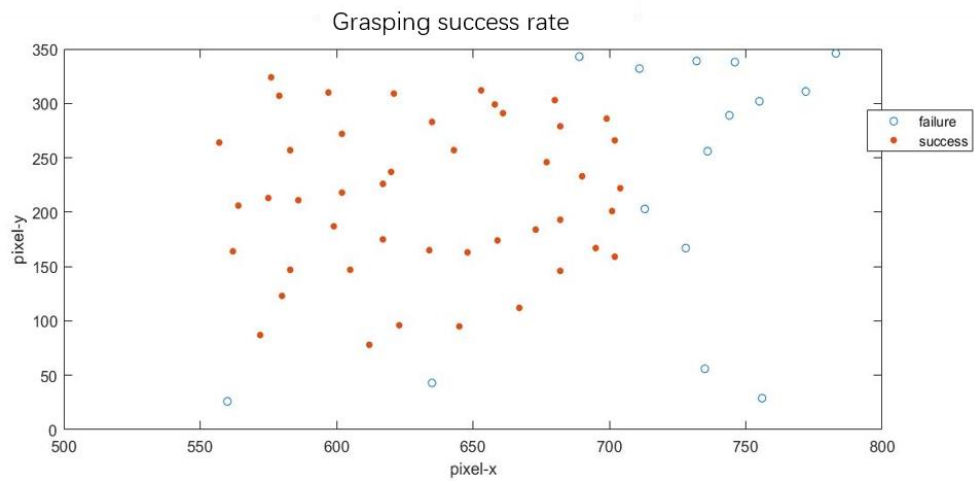


Figure 10. Success rate of grasping by the original gaussian model.

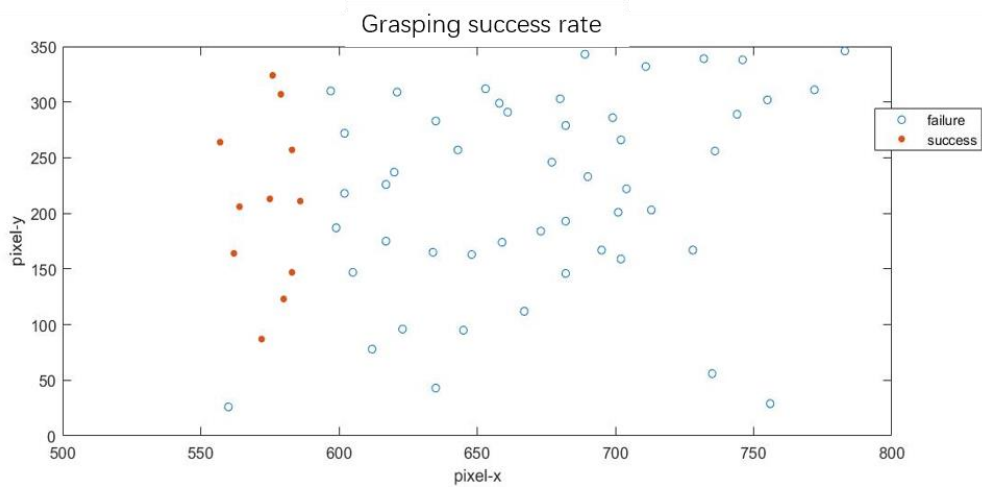


Figure 11. Success rate of VREP-based grasping simulation.

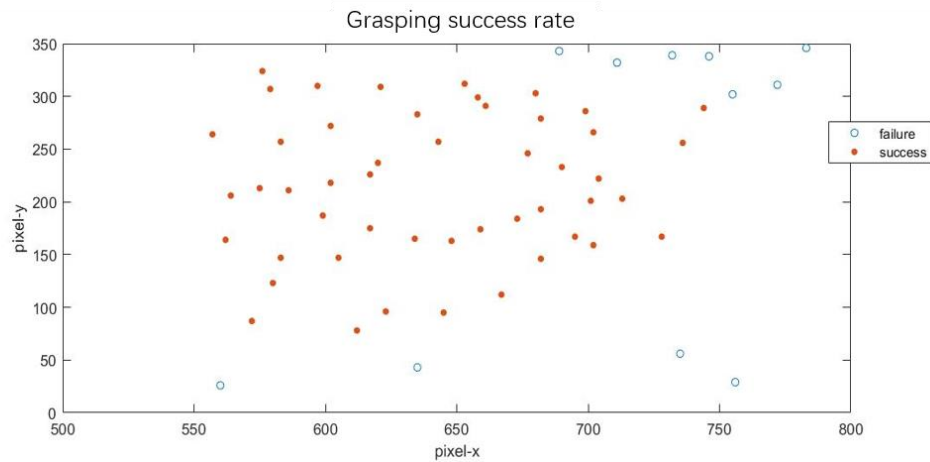


Figure 12. Success rate of grasping by the improved gaussian model.

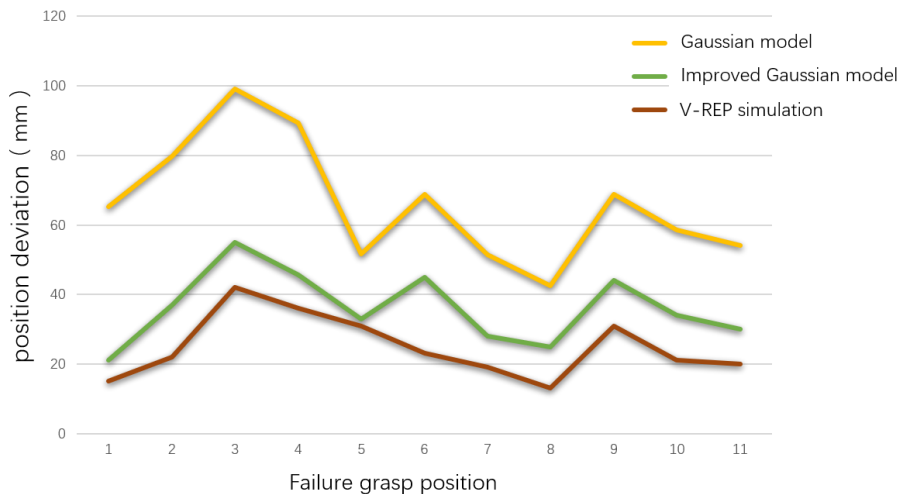


Figure 13. Analysis of positional deviations in areas of failed grasping.

Sixty points of the new area were randomly selected for testing, the test results are shown in Figure 10–12. The red solid circles indicated successful grasping and the hollow circles reflected failed grasping. According to the results, the success rate of direct grasping by the original Gaussian model was only 18.3%. The points for successful grasping were consisted in adjacency to the original area. The success rate of grasping by VREP-based simulations and improved Gaussian model was 81.7%, while the success rate of grasping by the improved Gaussian model was 75%. The success rate of the improved Gaussian model was slightly lower than the success rate of the simulation, possibly due to the errors in the precision of the camera sensor and robotic arm. This suggested that the improved Gaussian model could achieve more desirable grasping results in untrained areas after a minority of samples were updated.

In addition, we analysed the positional deviations for the 11 points where the grasping failed in any of the three methods. We got their positional deviation (Δd) between the statistical points and gripper end, as shown in Figure 13. It was observed that the displacement deviation was the highest

in the original Gaussian model, displacement deviation of the improved Gaussian model was higher than that of V-REP simulation but far lower than that of the original Gaussian model. This indirectly suggested that the improved Gaussian model was much more adaptive than the original model even in areas where grasping failed.

5. Conclusion

In this paper, a robotic grasping method based on the improved Gaussian model was put forward. This method was effective for grasping, as like the Gaussian models. It associated the observable variables with joint angles, trained areas with a minority of samples and successfully predicted the grasping at points of training areas without calibrating the visual systems. Unlike the original Gaussian model which was ineffective for predicting grasping results outside training areas, the improved model predicted grasping and achieved desirable results only by upgrading a minority of samples without any need for training samples in large areas. Finally, comparative tests were performed on real grasping, VREP-based grasping simulations by the improved Gaussian model and positional deviation analysis on areas of failed grasping. The experimental results validated the effectiveness of the method proposed in this paper.

Conflict of Interest

The authors declare there is no conflict of interest.

References

1. Y. Tao, T. Wang, H. Liu, S. Jiang, Insights and suggestions on the current situation and development trend of intelligent robots, *Chin. High Technol. Lett.*, **29** (2019), 149–163.
2. Z. Zhang, A flexible new technique for camera calibration, *IEEE Trans. Pattern Anal. Mach. Int.*, **22** (2000), 1330–1334.
3. Y. Wang, C. Liu, X. Yang, Online calibration techniques of visual measurement systems for industrial robots, *Robot*, **33** (2011), 299–302.
4. L. Zhang, X. Huang, W. Feng, Space robot vision calibration with reference objects from motion trajectories, *Robot*, **38** (2016), 193–199.
5. B. Belzile, L. Birglen, A compliant self-adaptive gripper with proprioceptive haptic feedback, *Auton. Rob.*, **36** (2014), 79–91.
6. D. Petković, M. Issa, N. D. Pavlović, L. Zentner, Ž. Čojbašić, Adaptive neuro fuzzy controller for adaptive compliant robotic gripper, *Expert Syst. Appl.*, **39** (2012), 13295–13304.
7. A. Ahrary, R. D. A. Ludena, A novel approach to design of an underactuated mechanism for grasping in agriculture application, in *Lee R. (eds) Applied Computing and Information Technology (eds. R. Lee)*, Springer, (2014), 31–45.
8. M. Manti, T. Hassan, G. Passetti, N. d'Elia, M. Cianchetti, C. Laschi, An underactuated and adaptable soft robotic gripper, in *Conference on Biomimetic and Biohybrid Systems*, Springer, (2015), 64–74.
9. C. Qian, R. Li, B. Li, M. Hu, Y. Xin, Study on bionic manipulator based on multi-sensor data Fusion, *Piezoelectr. Acoustoopt.*, **39** (2017), 490–493.

10. S. Liu, J. Deng, Y. Zhan, Y. Ye, Design and implementation of manipulator based on PWM technology, *J. Detect. Control*, **39** (2017), 19–23.
11. A. Saxena, J. Driemeyer, A. Y. Ng, Robotic grasping of novel objects using vision, *Int. J. Rob. Res.*, **27** (2008), 157–173.
12. W. Dong, Research on industrial robots scraping technologies based on machine vision, *Huazhong University of Science and Technology*, (2011).
13. Z. Yan, X. Du, M. Cao, Y. Cai, T. Lu, S. Wang, A method for robotic grasping position detection based on deep learning, *Chin. High Technol. Lett.*, **28** (2018), 58–66.
14. J. Xia, K. Qian, X. Ma, H. Liu, Fast planar grasp pose detection for robot based on cascaded deep convolutional neural networks, *Robot*, **40** (2018), 794–802.
15. Y. Mollard, T. Munzer, A. Baisero, M. Toussaint, M. Lopes, *Robot programming from demonstration, feedback and transfer*, 2015 IEEE/RSJ international conference on intelligent robots and systems (IROS), 2015. Available from: <https://ieeexplore.ieee.org/xpl/conhome/7347169/proceeding>.
16. K. Bousmalis, A. Irpan, P. Wohlhart, Y. Bai, M. Kelcey, M. Kalakrishnan, *Using Simulation and Domain Adaptation to Improve Efficiency of Deep Robotic Grasping*, 2018 IEEE International Conference on Robotics and Automation (ICRA), 2018. Available from: <https://ieeexplore.ieee.org/xpl/conhome/8449910/proceeding>.
17. M. Schwarz, C. Lenz, G. M. García, S. Koo, A. S. Periyasamy, M. Schreiber, *Fast Object Learning and Dual-arm Coordination for Cluttered Stowing, Picking, and Packing*, 2018 IEEE International Conference on Robotics and Automation (ICRA), 2018. Available from: <https://ieeexplore.ieee.org/xpl/conhome/8449910/proceeding>.
18. P. Schmidt, N. Vahrenkamp, M. Wächter, T. Asfour, *Grasping of Unknown Objects Using Deep Convolutional Neural Networks Based on Depth Images*, 2018 IEEE International Conference on Robotics and Automation (ICRA), 2018. Available from: <https://ieeexplore.ieee.org/xpl/conhome/8449910/proceeding>.
19. G. Zhao, Y. Tao, H. Liu, X. Deng, Y. Chen, H. Xiong, A robot demonstration method based on LWR and Q-learning algorithm, *J. Int. Fuzzy Syst.*, **35** (2018), 35–46.
20. Y. Chen, J. Guo, Y. Tao, Adaptive grasping strategy of robot based on Gaussian process, *J. Beijing Univ. Aeronaut. Astronaut.*, **43** (2017), 1738–1745.
21. E. Rohmer, S. P. N. Singh, M. Freese, *V-REP: A Versatile and Scalable Robot Simulation Framework*, 2013 IEEE/RSJ International Conference on Intelligent Robots and System, 2013. Available from: <https://ieeexplore.ieee.org/xpl/conhome/6679723/proceeding>.
22. N. Diego, *Virtual robot experimentation platform user manual [EB/OL]*, 2016. Available from: <http://www.coppeliarobotics.com/helpFiles/index.html>.
23. R. Iernsalimschy, *Programming in Lua*, Beijing: Publishing House of Electronics Industry, (2008).



AIMS Press

©2020 author name, licensee AIMS Press. This is an open access article distributed under the terms of the Creative Commons Attribution License (<http://creativecommons.org/licenses/by/4.0>)